INTRODUCTION

The work described herein was performed at the School of Aerospace Engineering, Georgia Institute of Technology during the period 12 February 1986 - September 1988. Professors Erian A. Armanios and Lawrence W. Rehfield were the Principal Investigators.

This research concerns the analysis and prediction of delamination damage that occur in composite structure on the on the sublaminate scale --that is the scale of individual plies or groups of plies. The objective have been to develop analytical models for mixed-mode delamination in composites. These includes:

(1) the influence of residual thermal and moisture strains
(2) local or transverse crack tip delamination originating at the tip of transverse matrix cracks
(3) delamination in tapered composite under tensile loading.

Computer codes based on the analytical models in (1) and (2) have been developed and comparisons of predictions with available experimental and analytical results in the literature have been performed. A simple analysis for item (3) has been developed and comparisons of predictions with finite element simulation is underway.

The usual approach to dealing with localized phenomena is large scale numerical simulation and analysis, mostly by general purpose finite element codes. This approach is often supplemented by a "build and test" demonstration, or series of demonstrations if repeated failures are encountered. While such approaches are often costly and inefficient, their major drawback is that fundamental principles are not discovered which provide the means to produce better results. Furthermore, the steps must be repeated all over again the next time a similar situation arises.

Overview of the Research

The research program can be separated into three elements: The influence of residual thermal and moisture stresses on the mixed-mode edge delamination of composites. The analyses of transverse crack-tip delamination and delamination analysis in tapered laminates under tensile loading. A detailed account of the analysis and applications of each element is provided in Appendices I through III. A brief description and summary of the major findings of each research element is presented in the following sections.

Influence of Hygrothermal Stresses

The sublaminate edge delamination analysis and code which had its origin in the research conducted under the earlier grant NAG-1-558 has been modified to include the effects of hygrothermal stresses.

The model is applied to mixed mode edge delamination specimens made of T300/5208 graphite/epoxy material. Residual thermal and moisture stresses significantly influenced the strain energy release rate and interlaminar stresses. Both experienced large increases when thermal conditions were added to the mechanical strains. These effects were alleviated when moisture stresses were included. Thermal effects on the interlaminar shear stress and total energy release rate were totally alleviated for the same specific moisture content. Moreover, this value of moisture content was not significantly affected by the stacking sequence for the laminates considered. This work is presented in accomplishments 3,4 and 12. A complete derivation of the analytical model, Fortran program listing and applications are provided in a accomplishment 3 and Appendix I.

Transverse Crack Tip Analysis

Transverse crack tip delaminations originate at the tip of transverse matrix cracks. This situation appears in Figure 1 where a symmetric laminate made of 90° plies in the core region and angle plies in the top and bottom portions is subjected to a tensile loading. Under tensile loading transverse

matrix cracks initiate in the core region reaching a saturation level at a crack spacing denoted by λ in the figure. Delamination often initiate at the tip of these transverse cracks. This situation is depicted in the generic model shown in Figure 1 of a symmetric delamination growing from a transverse crack tip.

Three analytical models, sublaminate shear, membrane and shear lag have been developed in order to estimate the saturated crack spacing distance. The saturation crack spacing corresponds to the distance from the crack where the broken plies regain their uniform stress/strain state i.e. where the interlaminar shear stress has decayed down to its far field (uniform) value. Based on the closed form expression for the interlaminar shear stress the crack spacing predicted by each model is presented in Table I. The experimental result in the table is based on Reifsnider's work for a $[0/90]_s$ laminate. A complete derivation of these models is provided in Appendix II.

The analysis of transverse crack tip delamination is presented in Appendix II and applied to $[\pm 25/90_n]$s laminates in the range n=0.5 to 8 made of T300/934 graphite/epoxy material. Closed form expressions for the interlaminar stresses, total strain energy release rate and energy release rate components are obtained. A computer code based on this analysis is developed and implemented into an earlier mixed-mode edge delamination code developed under the previous NASA grant NAG-1-558 and presented in accomplishment 6 and 7. This code was used to estimate the critical strain levels and the associated delamination damage mode with increasing number of 90° plies in the $[\pm 25/90_n]_s$. Since mid-plane edge delamination is a possible damage mode in this type of laminates a mid-plane delamination analysis was developed and presented in accomplishment 10. A computer code based on this analysis is developed and implemented in the mixed-mode edge delamination code. The critical strain and associated delamination damage modes predicted appear in Figure 2 and Table II. The critical stresses and associated delamination damage mode are provided in Table III.

Experimental results show that the local (crack tip) delamination phenomenon is the predominant damage mode only for n=4, 6 and 8 specimens. For n<4 edge delamination either in the mid-plane or in the 25/90 interface were observed in tests. The present analysis predicts mid-plane edge delamination for n=1/2 and 1 and mixed mode edge delamination for n=2 and 3, respectively. For n=4, 6 and 8 local delaminations are predicted to be the controlling damage mode with approximately 25 percent Mode II for the three specimens. The critical strains in Figure 2 and Table II are computed based on a fracture toughness values of 415 J/m^2, 140 J/m^2 and 120 J/m^2 for local delamination, mixed mode edge delamination and mid-plane edge delamination, respectively. A complete account of this work appears in Appendix II.

Analysis of Tapered Composites

A generic configuration of a tapered laminated composite is shown in Figure 3 where a 38 ply thick laminate is reduced to 26 ply by dropping three inner sets of plies. The basic analysis approach that is adopted utilizes two levels of modeling, a global scale and a local scale. The global scale is concerned with overall generalized forces and strains such as axial force and extension. A simple consistent deformation assumption is the foundation of this model. Global equilibrium equations are written and solved.

The generalized strains determined from the global analysis serve to provide estimates for the key primary stresses in the belt of the tapered section. Local estimates of interlaminar stresses are determined on the basis of equilibrium condition.

The total strain energy release rate is computed from the work done by the external applied loads. The work done by the external forces is based on the axial stiffness of the different elements in the tapered configurations. These elements are represented by the six sublaminates shown in Figure 4 where A_B denote the effective axial stiffness of the uncracked belt portion, A_{B1} the effective axial stiffness of the cracked belt portion. The uncracked belt portion in the tapered region makes an angle β with the loading axis while the

cracked portion makes an angle α due to delaminations along the taper and the uniform regions. These are denoted by a and b in Figure 4. The effective axial stiffness of the uncracked and cracked dropped plies are denoted by A_u and A_c respectively. The axial stiffness of the straight portion is denoted by A_s for the belt and A_f for the core plies.

The extent of delamination along the tapered and the uniform portion of the laminate has a significant influence on the axial stiffnesses A_u, A_c and A_{B1}. This is due to the discrete number of ply drops in the core region as illustrated in Figure 5 and the pop-off of the delaminated belt region.

A three-dimensional transformation is required in order to estimate the effective axial stiffness of the belt regions A_B and A_{B1}. This is due to the belt layup and the orientation of the different belt portions to the loading axis as shown in Figure 6.

The interlaminar stresses between the belt and the core plies are predicted by considering the equilibrium of the belt region. The equilibrium equations are derived using a complementary potential energy formulation of the belt on an elastic foundation. The elastic foundation is made of two contributions. The first, is a continuous shear restraint provided by the resin pocket regions at the interface between the belt and the inner core plies. The second, is a discrete number of concentrated transverse normal (R_i) and shear (T_i) forces at the ply drop locations as shown in figure 7 for i=1-4. The distributed shear stiffness is denoted by G in Figure 8 while the transverse normal and shear stiffnesses at the ply drop locations are denoted by k_i and g_i (i=1-4), respectively.

The variation of the total strain energy release rate G with delamination a growing along the tapered region appears in Figure 9. The effect of delamination b along the uniform portion on a is also shown in the figure. The discrete jumps at a/h equal 20 and 40 correspond to the ply drop. A plot of the concentrated transverse normal and shear forces and the interface between the belt and the inner core appears in Figure 10.

A detailed description of the analysis, closed form expressions for the total energy release rate and interlaminar stresses is provided in Appendix III. Additional refinements are planned within this general framework such as accounting for shear strains in the belt and increasing the number of sublaminate elements in the analysis.

ACCOMPLISHMENTS

Publications

1. Armanios, E.A. and Rehfield, L.W., "Interlaminar Analysis of Laminated Composites Using a Sublaminate Approach," Proceedings of the AIAA/ASME/ASCE/AHS 27th Structures, Structural Dynamics, and Materials (SDM) Conference, San Antonio, Texas, 19-21 May, 1986. AIAA Paper No. 86-0969CP, Part 1, pp. 442-452.

2. Rehfield, L.W., Armanios, E.A. and Weinstein, F., "Analytical Modeling of Interlaminar Fracture in Laminated Composites," Composites '86: Recent Advances in Japan and the United States, Proceedings of the Third Japan-U.S. Conference on Composite Materials, K. Kawata, S. Umekawa, and A. Kobayashi Eds., 1986 pp. 331-340.

3. Mahler, M.A., "A Study on the Thermal and Moisture Influences on the Free-edge Delamination of Laminated Composites," Special Problem in Partial Fulfillment for M. Sc., School of Aerospace Engineering, Georgia Institute of Technology, September, 1987.

4. Armanios, E.A. and Mahler, M.A., "Residual Thermal and Moisture Influences on the Free-Edge Delamination of Laminated Composites," Proceedings of the AIAA/ASME/ASCE/AHS 29th Structures, Structural Dynamics and Materials (SDM) Conference, Part 1, pp. 371-381, 1988.

5. Armanios, E.A. and Rehfield, L.W., "Interlaminar Fracture Analysis of Composite Laminates Under Bending and Combined Bending and Extension," Composite Materials: Testing and Design (Eighth Conference), ASTM STP 972, J. D. Whitcomb, Eds., American Society for Testing and Materials, Philadelphia, 1988, pp. 81-94.

Publications Pending

6. Armanios, E.A. and Rehfield, L.W., "Sublaminate Analysis of Interlaminar Fracture in Composites: Part I-Analytical Model," Journal of Composites Technology and Research, July, 1988.

7. Armanios, E.A., Rehfield, L.W., Raju, I.S. and O'Brien, T.K.," Sublaminate Analysis of Interlaminar Fracture in Composites: Part II - Applications," Journal of Composites Technology and Research, July, 1988.

8. Armanios, E.A. and Rehfield, L.W., "A Simplified Approach to Strain Energy Release Rate Computations for Interlaminar Fracture of Composites," Composites '88: Recent Advances in Japan and the United States, Proceedings of the Fourth Japan - U.S. Conference on Composite Materials.

9. Sriram, P. and Armanios, E.A., "Fracture Analysis of Local Delaminations in Laminated Composites," to appear in the proceedings of the AIAA/ASME/ASCE/AHS/ASC 30th Structures, Structural Dynamics and Materials (SDM) Conference, April, 1989.

10. Armanios, E.A., Sriram, P. and Badir, A., "Sublaminate Analysis of Mode I Edge Delamination in Laminated Composites," to appear in the proceedings of the AIAA/ASME/ASCE/AHS/ASC 30th Structures, Structural Dynamics and Materials (SDM) Conference, April, 1989.

Presentations

11. Armanios, E.A. and Mahler, M.A., "Residual Thermal and Moisture Influences on the Free-edge Delamination of Laminated Composites," presented at the 29th Structures, Structural Dynamics and Materials (SDM) Conference, Williamsburg, VA, April 18-20, 1988.

Table I Comparison of Transverse Crack Spacing

Model		Saturated Crack Spacing (mm)
Shear	2 Sublaminates	1.651
	4 sublaminates, $a \rightarrow 0$	1.105
Membrane		1.004
Shear Lag		1.160
Experimental		1.131

Table II Critical Strains and Associated Delamination Damage Modes

Critical Strains (%)

Number of 90° plies	Experimental	Local Delamination	Edge Delamination	
			Mixed Mode	Mid-Plane
1/2	0.6058	1.6747	0.6819	0.6058
1	0.5936	1.1685	0.6262	0.5677
2	0.5934	0.8058	0.5964	0.6402
3	0.5934	0.6427	0.5862	0.7582
4	0.5369	0.5444	0.5810	0.8815
6	0.3914	0.4264	0.5757	1.1133
8	0.3589	0.3555	0.5731	1.3199

Table III Critical Stresses and Associated Delamination Damage Modes

Critical Stresses (MPa)

Number of 90° plies	Experimental	Local Delamination	Edge Delamination	
			Mixed Mode	Mid-Plane
1/2	438	1313.9	535.0	475.3
1	409	784.0	420.1	380.9
2	324	426.2	315.4	338.6
3	270	285.1	260.1	336.4
4	211	210.6	224.7	341.0
6	128	134.7	181.8	351.6
8	94.4	97.1	156.6	360.5

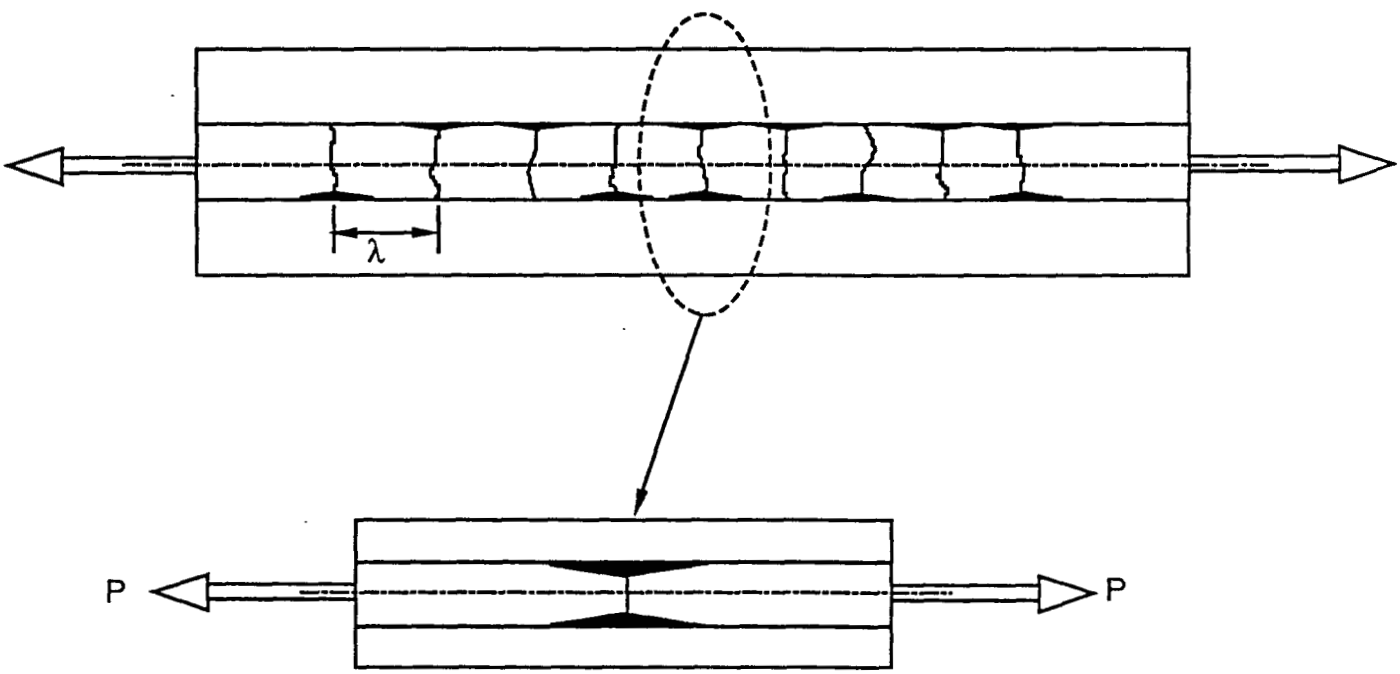

Fig. 1 Generic Crack-tip Delamination

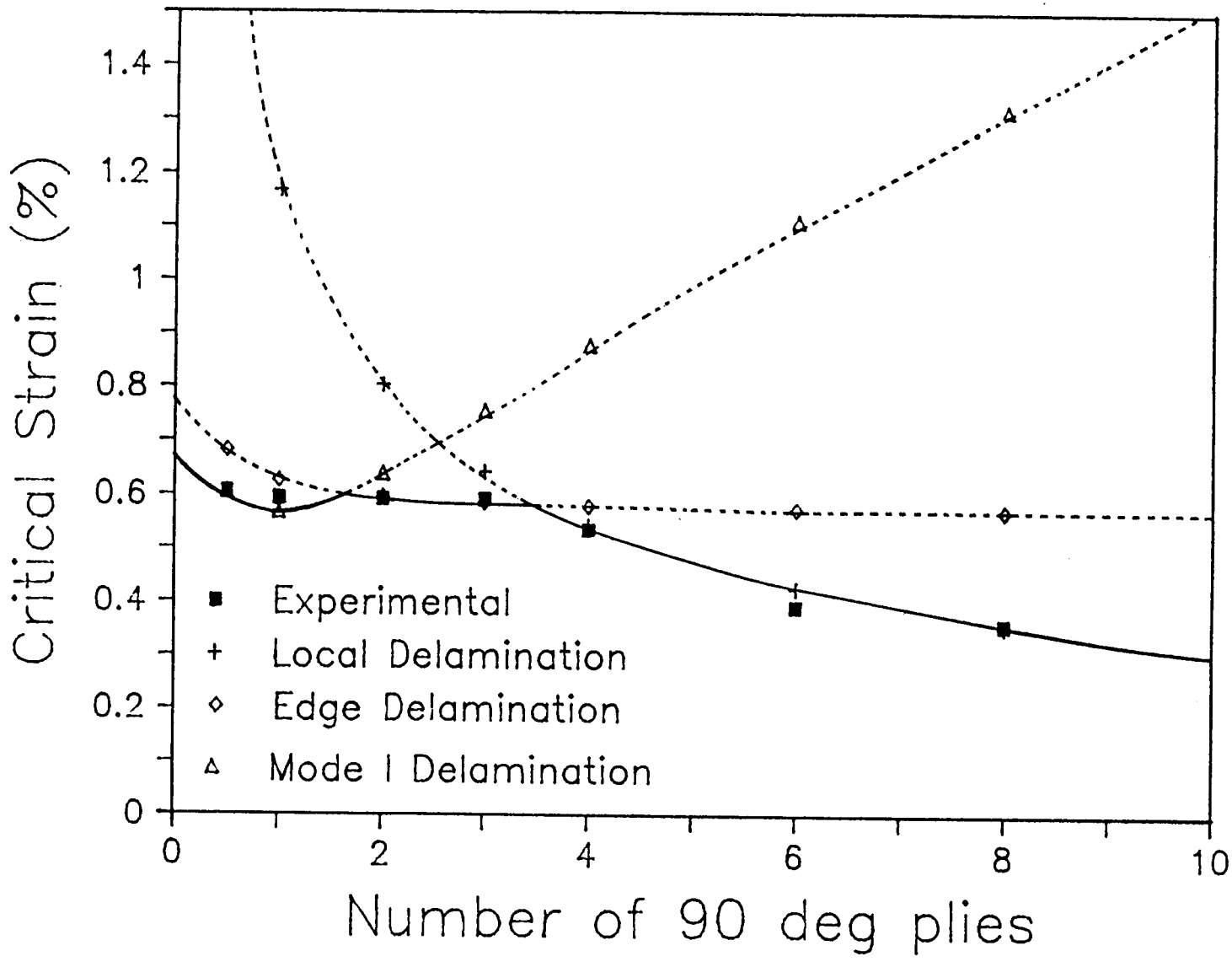

Fig. 2 Critical Strains and Associated Delamination Damage Modes

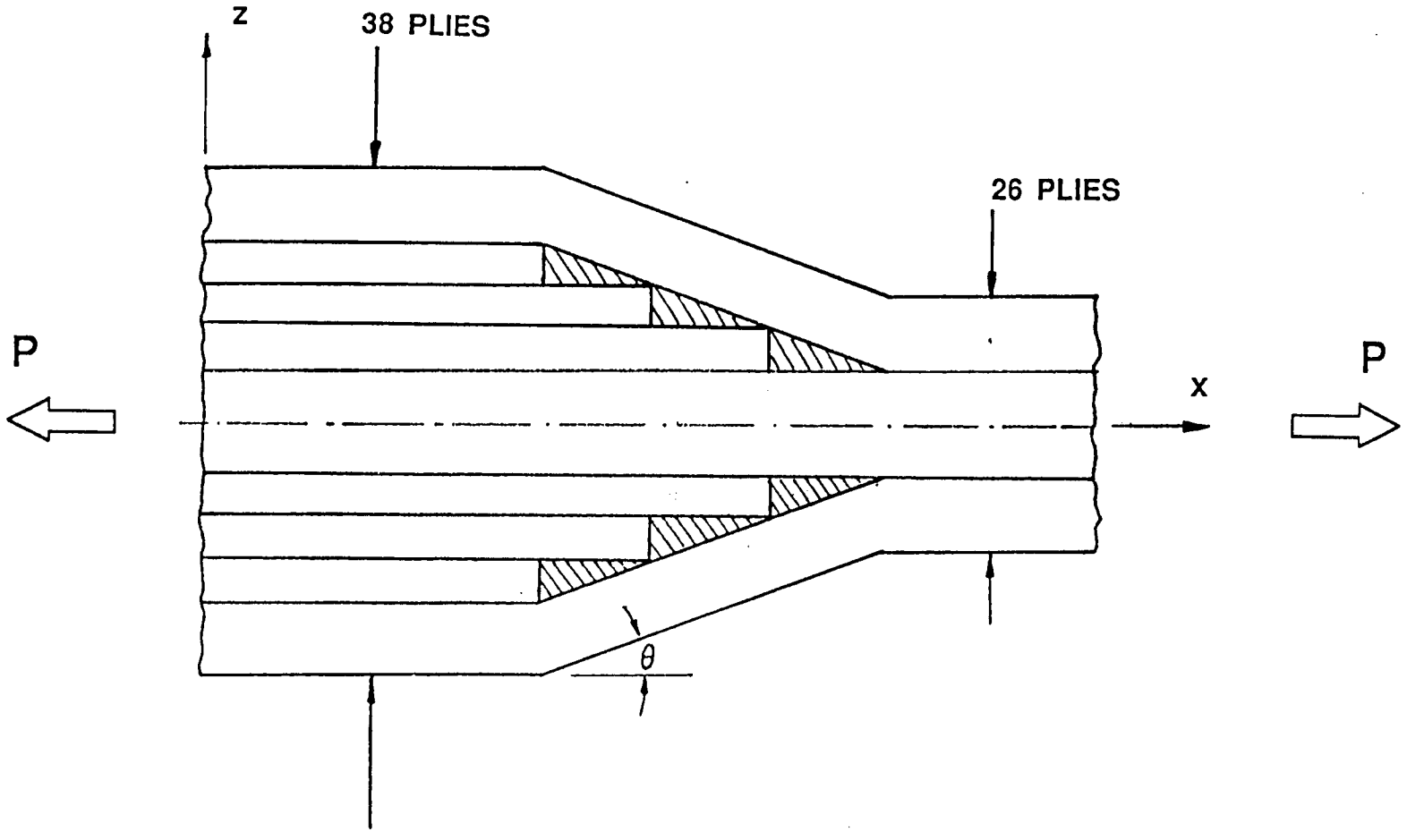

Figure 3. Edge View of the Tapered Structure

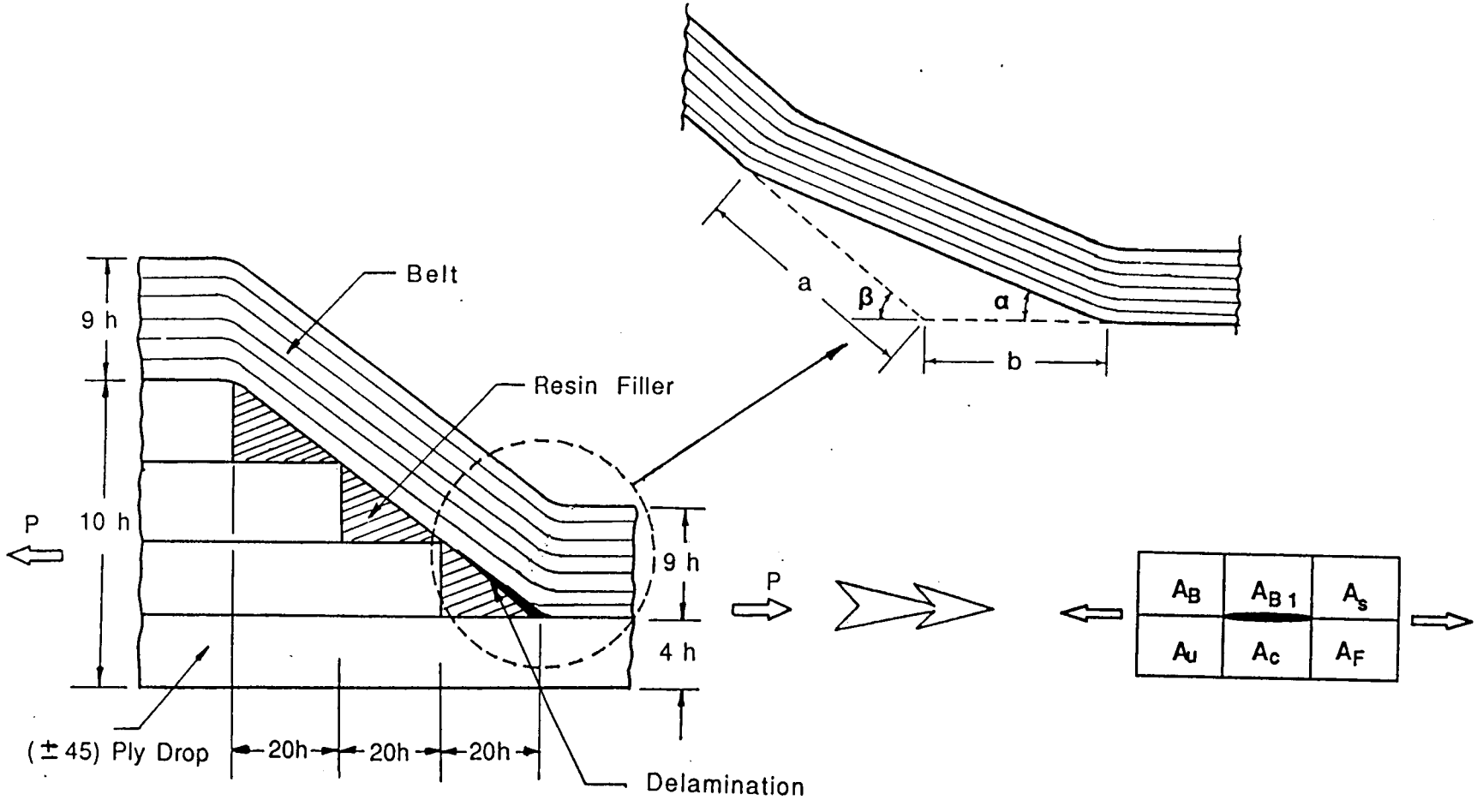

Figure 4. Modelling Approach

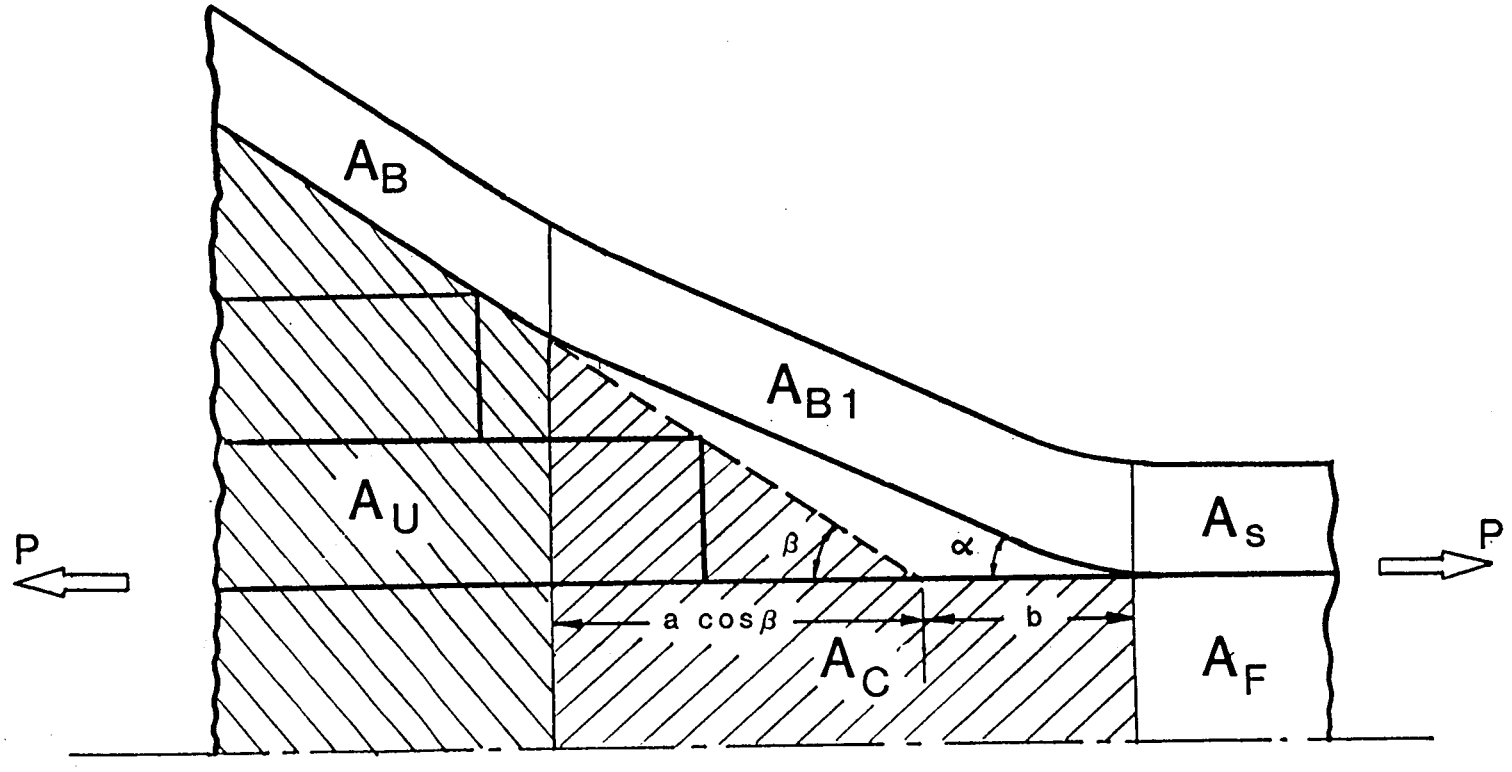

Figure 5. Dependency of Core and Belt Stiffnesses on Delamination

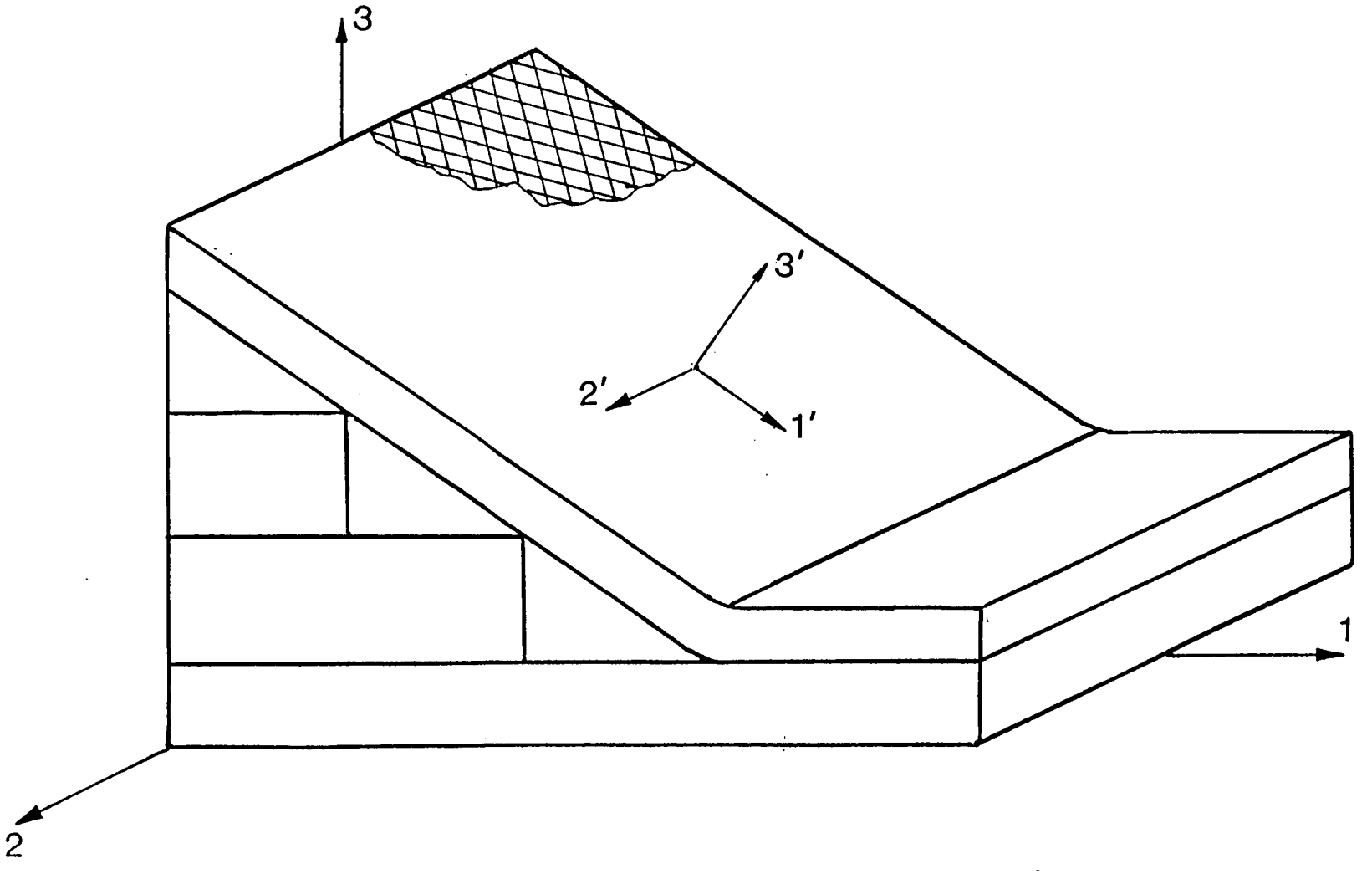

Figure 6. Three Dimensional Coordinates in the belt Region

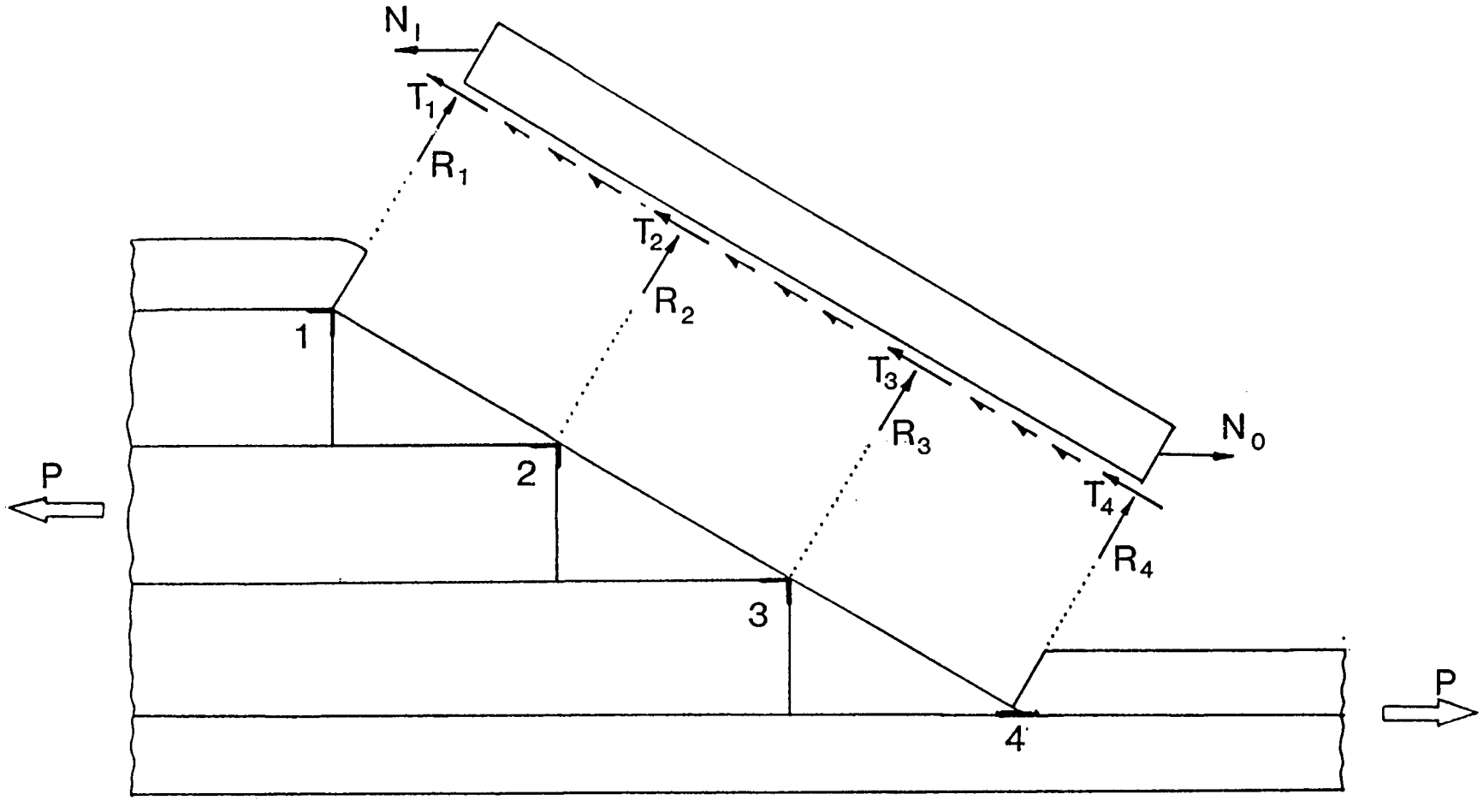

Figure 7. Interlaminar Stresses

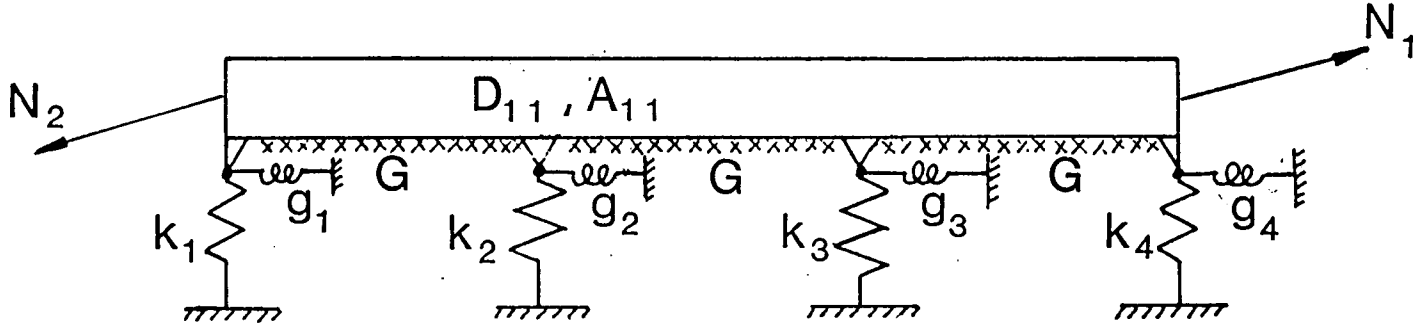

Figure 8. Elastic Stiffnesses and Supporting Conditions

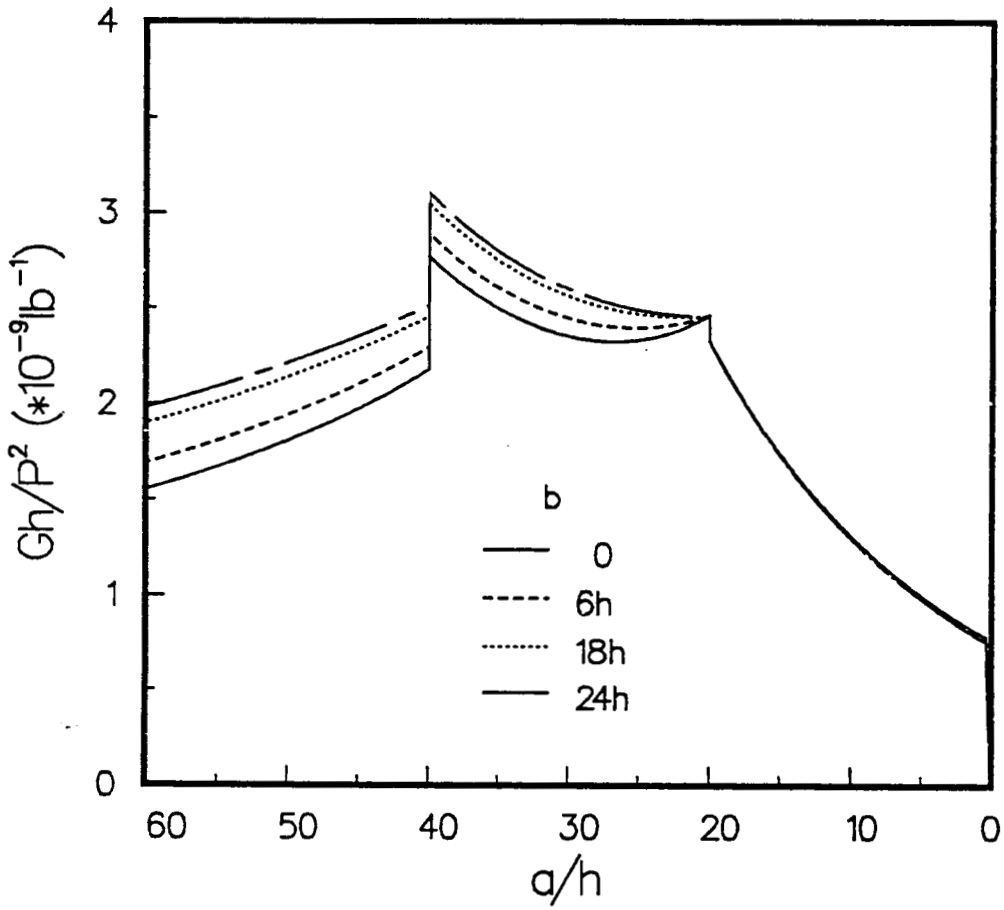

Figure 9. Variation of Total Strain Energy Release Rate with Delamination

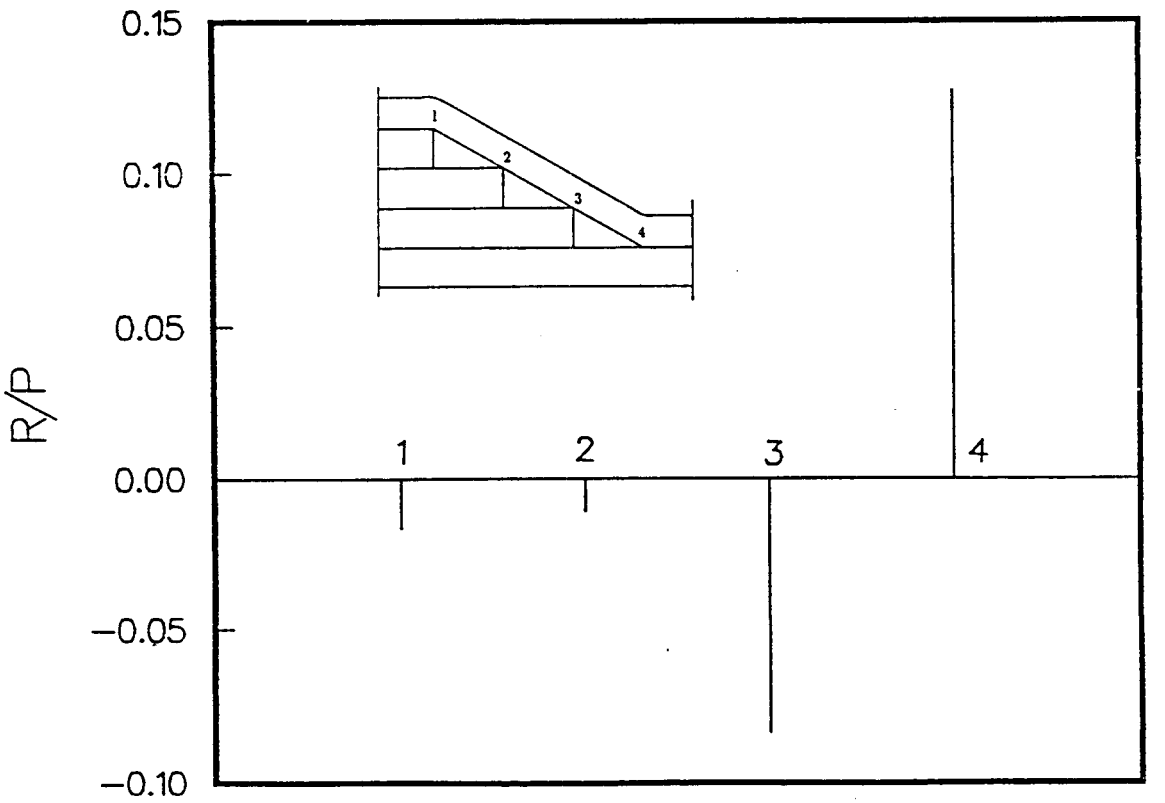

Figure 10 a. Distribution of Concentrated Normal Forces Along the Belt

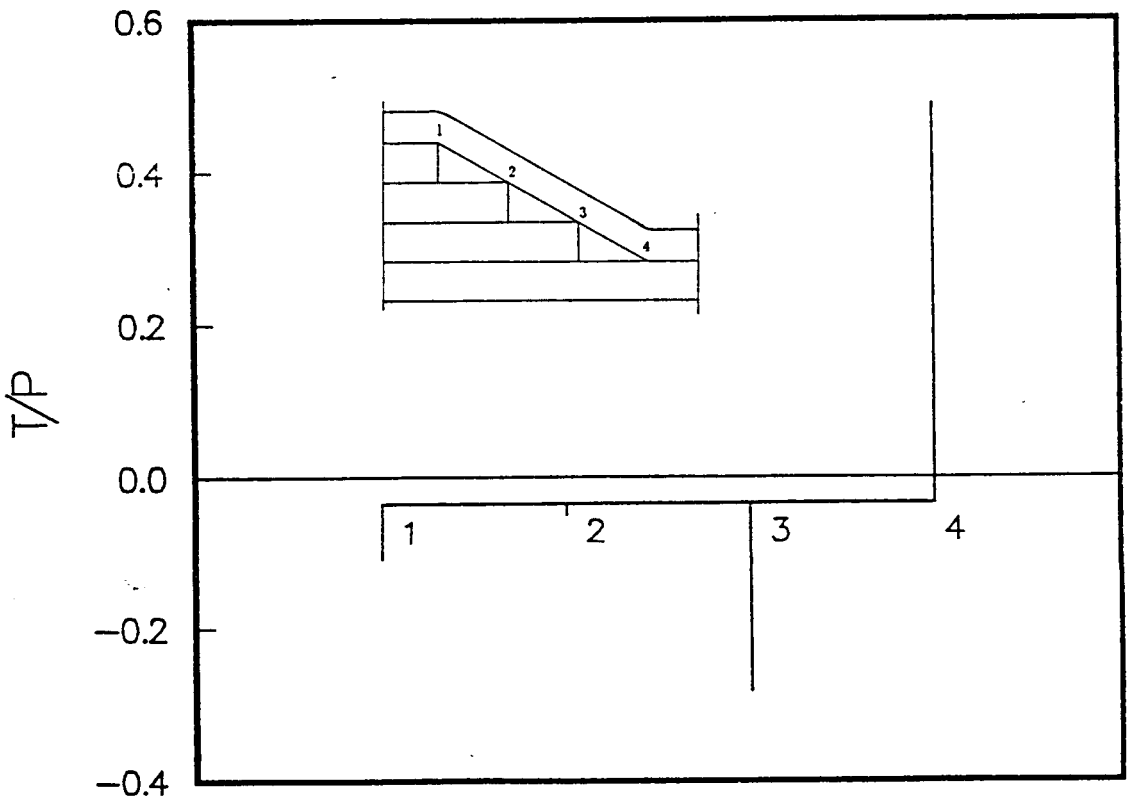

Figure 10 b. Distribution of Concentrated Shear Forces Along the Belt